https://doi.org/10.5194/egusphere-2026-1498
Preprint. Discussion started: 8 April 2026

Forecasting the Flame: Simulating Future Wildfire Regimes in the Northeast Mediterranean

Bikem Ekberzade[1]

[1]Istanbul Technical University, Eurasia Institute of Earth Sciences, Istanbul, Turkey

Correspondence to: Bikem Ekberzade (ekberzade19@itu.edu.tr)

ORCID: 0000-0002-3271-2040

Abstract. Despite a global decline in total burned area, high-impact wildfire events continue to pose growing threats to ecosystems and human communities. As climate change amplifies hydroclimatic extremes, cycles of precipitation-driven fuel build-up followed by persistent drought are increasing the likelihood of severe wildfires. Moving beyond estimates of total burned area, this study aims to answer "where, and how often, will future landscapes burn?" by quantifying wildfire hazard through fire probability and fire return intervals for the northern segment of the Eastern Mediterranean Basin (34–46°N, 24–50°E), a region where such extremes are expected to fundamentally alter fire regimes. Potential changes in fire activity were investigated for the period 1961–2100 using the process-based dynamic vegetation model LPJ-GUESS coupled with SIMFIRE–BLAZE wildfire modules. Terrestrial vegetation was represented using regionally parameterized Plant Functional Types, and simulations were forced with ERA5-Land reanalysis for the historical period (1961–2025) and an ensemble of five CMIP6 climate projections under a high-emissions scenario (SSP5-8.5) for exploratory future analysis (2015–2100). Benchmarking against MODIS MCD64A1 observations revealed that while the model successfully reproduced domain-scale burned area magnitudes and interannual variability, weak spatial agreement highlighted the strong influence of localized anthropogenic ignition and suppression processes not represented in the natural-potential experimental design. Future projections indicated that changes in fire probability and return intervals are unlikely to be spatially uniform. Instead, simulation results highlight a fundamental reorganization of fire regimes driven by the interplay between hydroclimatic change, vegetation dynamics, and landscape structure. By combining temporally explicit reanalysis data with ensemble climate projections, this study distinguishes between the role of observed hydroclimatic extremes in shaping historical fire activity and the importance

https://doi.org/10.5194/egusphere-2026-1498
Preprint. Discussion started: 8 April 2026

of long-term climate trajectories in constraining future risk. The findings suggest that climate change may not simply increase overall wildfire activity, but rather systematically redistribute fire risk across the region, with urgent implications for anticipating emerging hotspots and adapting fire management strategies.

1. Introduction

As the effects of climate change intensify, large and severe wildfire episodes with significant socio-economic and ecological impacts continue to dominate global headlines. In January 2025 alone, the fatal Palisades and Eaton Fires devastated close to 38,000 ha of natural habitat and human settlements in the United States (CAL FIRE, 2025; WWA, 2025a), while during the subsequent summer months widespread wildfire activity across Portugal, Spain, Greece, Cyprus, and Türkiye continued to claim lives (Keeping et al., 2025; WWA, 2025b). Regardless of fire suppression efforts or the fire-adapted traits of many Mediterranean taxa, projected increases in the frequency and severity of disturbances under climate change, combined with the rapid expansion of the wildland–urban interface (WUI), are expected to exacerbate future wildfire hazard and uncertainty (Gonzalez and Ghermandi, 2024; Wasserman and Mueller, 2023). As a result, anticipating potential fire episodes and constructing plausible “wildfire trajectories” for densely populated regions with seasonal wildfire activity have become growing priorities from scientific, policy, and humanitarian perspectives.

While excess heat, fuel abundance, prolonged drying, and strong airflow are required for a high-severity wildfire (Newman Thacker, 2025), two overarching drivers – often operating in tandem – set the stage for megafires: ignitions, which are predominantly human-caused (Ekberzade et al., 2025; Ellis et al., 2025; Gelabert et al., 2025), and climate change. Although the former can be identified through forensic analyses, climate change has been robustly linked to the intensification of wildfire activity by expanding the amplitude of climatic variability (François et al., 2025; Wood, 2023) and amplifying hydroclimatic extremes (Sutanto et al., 2025; Richardson et al., 2022). This relationship has been particularly evident during recent fire seasons, including the extreme wildfire outbreaks in southern Europe in 2021 (San Miguel-Ayanz et al., 2022; Duane et al., 2021), and in Cyprus, Greece and Türkiye in 2025 (WWA, 2025b).

Much as human behavior is complex and human ignitions remain difficult to predict, analyses of climate variability and burned area (BA) based on large-scale remote sensing and observational datasets can

https://doi.org/10.5194/egusphere-2026-1498
Preprint. Discussion started: 8 April 2026

provide valuable insights into regions exhibiting persistent fire activity. Such analyses can identify active pyro-catchments, characterized by spatial persistence in BA (Ekberzade et al., 2025), as well as potential wildfire hotspots associated with temporal persistence. Process-based dynamic global vegetation models (DGVMs) coupled with fire modules offer a complementary framework for exploring how these fire-prone regions may respond to future climate change. By explicitly linking climate drivers with vegetation dynamics, coupled DGVMs enable the investigation of how fuel accumulation and burn potential – and, consequently, regional fire regimes – may evolve over time under different climate scenarios (Nurrohman et al., 2024; Pellegrini et al., 2023). Together, these approaches provide critical guidance for policymakers seeking to implement preventive measures and for first responders planning targeted interventions in high-risk areas ahead of the fire season.

This study presents simulations from the process-based dynamic vegetation model LPJ-GUESS, coupled with fire and combustion modules and driven by high-resolution reanalysis data and bias-corrected global climate model (GCM) outputs. Model simulations are synthesized with observational records, including satellite-derived burned area and climate indices such as the Standardized Precipitation-Evapotranspiration Index (SPEI), to evaluate the model's capacity to reproduce historical fire dynamics and distinguish natural, climate-driven fire potential from anthropogenic influences over the historical period (1961–2025). Building on this evaluation, an ensemble of future projections under the high-emissions SSP5-8.5 scenario is used to explore ecosystem responses to strong warming and drying conditions through the end of the century (2015–2100). These simulations investigate whether such climate trajectories will simply intensify existing wildfire activity or drive a fundamental spatial reorganization of fire regimes across the region.

2. Methodology

2.1 Study area

The study area is situated in the northern segment of the Eastern Mediterranean Basin. It centers on the Anatolian Peninsula, also covering its immediate surroundings between 34–46°N and 24–50°E. The Anatolian Peninsula is a high plateau with elevations increasing from the Aegean coast in the west towards the eastern highlands. Two mountain ranges in the north and the south block most of the maritime effect from both seas from entering inland, creating a semi-arid continental climate in the inner peninsula. The

https://doi.org/10.5194/egusphere-2026-1498
Preprint. Discussion started: 8 April 2026

coastal climates are mainly Mediterranean. In the northeast, there is a temperate rainforest belt that extends along the Black Sea coast towards the Caucasus Mountains. In the south, the Taurus Mountain Range continues to become the Zagros Mountains, where the East Anatolian deciduous forest ecoregion turns into montane steppes which continue for the greater part of this semi-arid mountain range.

The different climate and vegetation patterns of the study area create different fire histories. In certain places where vegetation forms dense canopies, the precipitation patterns may keep fire return intervals high (FRI ≥ 50 yr), such as in the southeastern Black Sea coast (northern Anatolia). In others, seasonality and aridity may encourage frequent burns. In zones where fire frequency is high (FRI is low), most woody taxa are not only adapted to, but also dependent on fire to survive (e.g., Mediterranean shrubs and certain pine species that are serotinous).

The region also bears a strong human imprint on the landscape. Large portions of Central Anatolia, the Pontic steppes, and the Caspian lowlands are dominated by croplands and heavily grazed rangelands. While agricultural expansion may amplify burned area in the observational record (through stubble burning, Fig. 1), grazing pressure and active fire suppression fragment natural fuel continuity and often reduce the spatial extent of large fires despite favorable climatic conditions. As a result, the observed fire regimes in

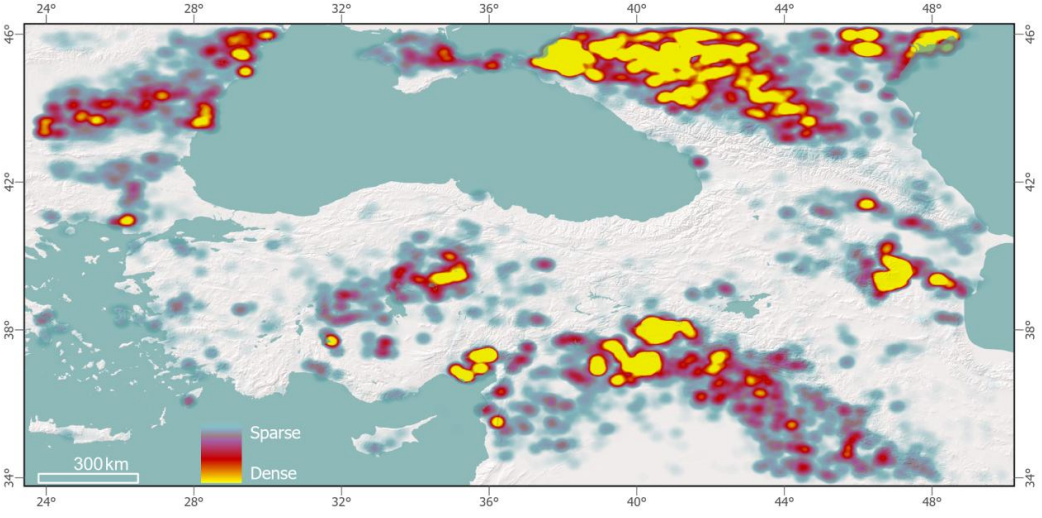

Figure 1. Wildfire hotspots within the study domain. The heatmap was created using MODIS MCD64A1 dataset for burned area between 2000 and 2025 (Giglio et al., 2021). Bright yellow marks indicate tight burned area clusters, or wildfire hotspots.

https://doi.org/10.5194/egusphere-2026-1498
Preprint. Discussion started: 8 April 2026

many semi-arid ecosystems reflect not only climatic constraints but also intensive land management. This anthropogenic modulation is particularly relevant for steppe environments, where fuel continuity and biomass accumulation can fluctuate strongly between years. Consequently, in these landscapes, the climatic fire potential simulated by dynamic vegetation models may show acute differences in burned area from those recorded by satellite observations (Ekberzade et al., 2025).

2.2 Dynamic vegetation and fire modeling framework

Burned area (BA) and fire return interval (FRI) were simulated using the process-based dynamic vegetation model LPJ-GUESS v.4.1 (Smith et al., 2001). The model was coupled with the SIMFIRE (Knorr et al., 2014) and BLAZE (Rabin et al., 2017) fire modules. In this configuration, SIMFIRE estimates the probability of fire occurrence based on biome type, climate conditions, and vegetation abundance, the latter proxied by the fraction of absorbed photosynthetically active radiation (FAPAR). Within the LPJ-GUESS patch framework, these probabilities are used to generate stochastic ignition events, from which the realized burned area fraction emerges as the proportion of burned patches within each grid cell. BLAZE then simulates the mechanistic impacts of these fires, including combustion-related mortality, biomass consumption, and carbon fluxes, based on explicit fuel loads and local fire weather conditions.

Forced with seven climate variables (mean, minimum, and maximum temperatures, precipitation, relative humidity, solar radiation, and wind speed), soil properties, and atmospheric CO_2 concentrations, the model simulates each grid cell independently. All simulations in this study were conducted at a daily temporal resolution, producing annual outputs of burned area, fire probability, and vegetation state variables. Regional model parameterization, plant functional type (PFT) settings, and other calibration choices followed those described in Ekberzade et al. (2024). To isolate the role of climate and vegetation in shaping potential fire regimes, anthropogenic ignitions and fire suppression were excluded, assuming fires arise exclusively from natural ignitions.

2.3 Experimental design

To characterize both current fire dynamics and potential changes in wildfire regimes, simulations were conducted in two stages: historical simulations and future projections. All post-simulation analyses were conducted using R and Python programming languages, Climate Data and NetCDF Operators (CDO/NCO).

https://doi.org/10.5194/egusphere-2026-1498
Preprint. Discussion started: 8 April 2026

2.3.1 Historical simulations and pattern evaluation (1961–2025)

In the first step, LPJ-GUESS coupled with SIMFIRE–BLAZE was forced with high-resolution reanalysis data for the historical period (1961–2025), and bias-corrected global climate model (GCM) datasets. These simulations were designed to assess the model's ability to reproduce observed spatial patterns and temporal variability of BA across the study region. Simulated BA, both from reanalysis and bias-corrected GCM datasets, was compared against satellite-derived burned area products using geospatial and statistical analyses.

Emphasis was placed on the spatial distribution and temporal variability of BA, rather than exact magnitudes, as even small anthropogenic interventions – which are absent in the experimental design – can produce disproportionately large observed burned areas (Ekberzade et al., 2025; Li et al., 2024; Hantson et al., 2016). Particular attention was given to natural vegetation zones, where natural ignitions are expected to drive fire activity more than anthropogenic ignitions (although the latter can still occur). Comparisons were performed for long-term means and interannual variability in burned area, allowing the identification of persistent wildfire hotspots and regions where simulated and observed fire patterns converged.

2.3.2 Future projections (1961–2100)

In the second step, an ensemble of simulations spanning 1961–2100 was conducted in which LPJ-GUESS was forced with bias-corrected, high-resolution global climate model (GCM) datasets. Bias correction was performed using the reference period 1995–2014, selected to represent contemporary climate conditions while overlapping with the observational period used for model evaluation. This ensures that the bias-corrected forcing reflects recent warming trends without relying on cooler late-20th-century climatologies. The SSP5-8.5 scenario was chosen as a high-end forcing pathway to explore the potential upper bound of climate-driven fire activity, intended as a stress test of ecosystem responses under strong warming and drying conditions rather than a deterministic prediction of future fire regimes. Simulation results were analyzed to examine potential changes in burned area, fuel availability (represented by FAPAR), and fire return intervals, with particular focus on fire-prone ecoregions and the emergence of new potential wildfire hotspots under strong warming and drying conditions.

https://doi.org/10.5194/egusphere-2026-1498
Preprint. Discussion started: 8 April 2026

2.3.3 Spatial aggregation and ecoregion framework

To evaluate model performance and characterize fire regime behavior across ecologically meaningful units, all analyses were conducted at the level of terrestrial ecoregions, since they delineate regions with relatively homogeneous climate, vegetation structure, fuel characteristics, and disturbance regimes, making them particularly suitable for fire-vegetation analyses. The Terrestrial Ecoregions of the World dataset by Dinerstein et al. (2017; data available from WWF, 2017) was selected as the primary spatial aggregation framework. A total of 29 of these ecoregions intersect the study area (Fig. 2). BA, vegetation, and fire regime metrics were aggregated annually within each ecoregion for both simulations and observations. Subsequent analyses focused on identifying ecoregions exhibiting persistent or recurrent fire activity (pyro-catchments), as well as those where fire occurrence is rare or episodic.

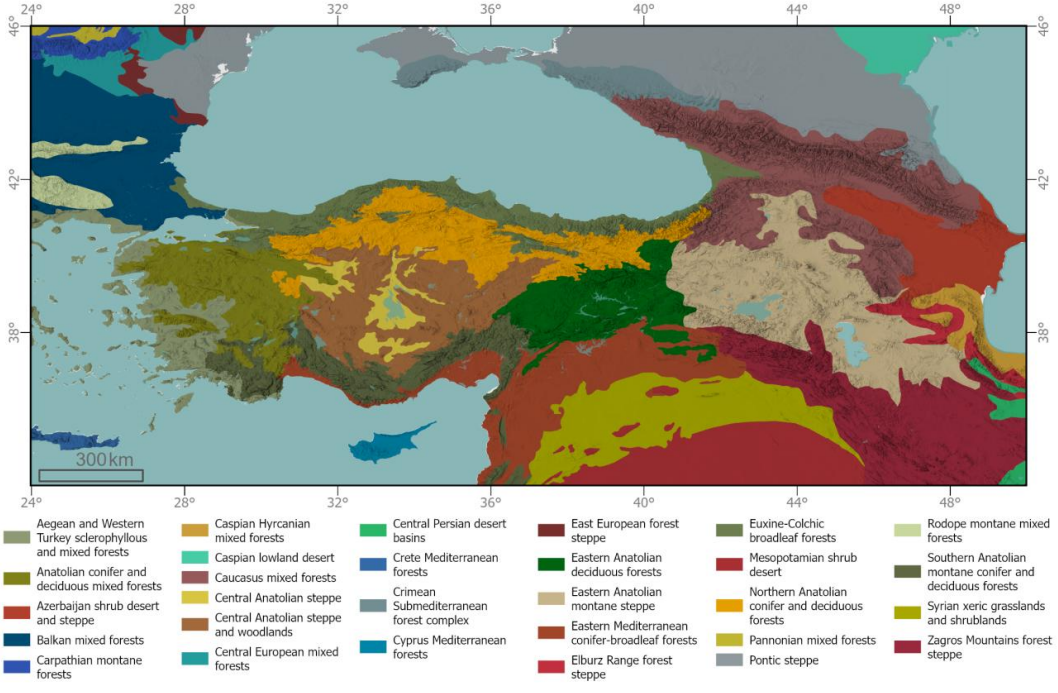

Figure 2. Ecoregions within the study area. The map is adapted from the dataset Terrestrial Ecoregions of the World (Dinerstein et al., 2017; data available from WWF, 2017), and shows the 29 ecoregions that were used as aggregation units in fire regime analyses. Note the diverse ecosystems in close proximity within the study domain.

2.3.4 Model evaluation and statistical analysis

https://doi.org/10.5194/egusphere-2026-1498
Preprint. Discussion started: 8 April 2026

Model performance was evaluated by comparing simulated BA from LPJ-GUESS–SIMFIRE–BLAZE against observed BA from the MODIS MCD64A1 dataset (Giglio et al., 2021). All datasets were aggregated to the 29 terrestrial ecoregions within the study domain to reduce scale mismatch between gridded model output and satellite observations. Annual BA was converted to square kilometers and normalized by ecoregion area to ensure comparability. Rather than pixel-level agreement, model evaluation focused on three complementary aspects of fire regime behavior: (1) spatial fire patterns across ecoregions, (2) interannual variability in burned area, and (3) persistence and dominance of high-fire years.

Spatial patterns were assessed by comparing long-term mean annual BA across ecoregions using Spearman rank correlation (ρ). This approach evaluates the model's ability to correctly rank fire-prone versus fire-limited ecoregions, independent of absolute BA magnitude. Interannual variability was quantified by calculating the Spearman correlation between observed and simulated annual BA for each ecoregion. The distribution of these correlations was summarized using boxplots to evaluate overall model skill in capturing climate-driven fire activity.

To characterize recurrent fire activity and identify potential pyro-catchments, fire persistence was quantified for each ecoregion as the fraction of years in which BA exceeded the upper quartile of the local BA distribution. Ecoregions were ranked by this persistence metric to distinguish structurally fire-prone regions from those experiencing infrequent or episodic fires. Together, these analyses provide a regime-based evaluation of model performance across ecologically distinct fire environments, rather than a point-by-point comparison of burned area magnitudes.

Finally, the representation of extreme fire activity was evaluated by identifying, independently for observations and simulations, the year of maximum annual BA within each ecoregion and computing the absolute difference in peak-fire timing.

2.4 Datasets

2.4.1 Climate datasets and bias correction

For the historical analysis (1961–2025), LPJ-GUESS was forced with ERA5-Land reanalysis data. For the simulations including future projections (1961–2100), to ensure the robust representation of climate

https://doi.org/10.5194/egusphere-2026-1498
Preprint. Discussion started: 8 April 2026

variability and extreme events – which are critical drivers of wildfire dynamics in the SIMFIRE-BLAZE module – outputs from five GCMs (CMIP6, SSP5-8.5) were interpolated to 0.1° resolution, and bias-corrected against the 1995–2014 ERA5-Land reference period using Quantile Delta Mapping (QDM). QDM preserves the GCM-projected relative or absolute changes in all quantiles while effectively correcting systematic historical biases relative to the observational baseline (Supplementary Table S1 and Figs. S1–S7). ERA5-Land reanalysis data (aggregated to daily minimum, mean, maximum, and sum for precipitation) were utilized as the historical reference dataset. Prior to correction, all GCM calendars were standardized to a Gregorian leap-year calendar to ensure exact day-to-day temporal alignment with the reference observations.

The QDM algorithm was tailored to the specific physical boundaries of each meteorological variable. For precipitation, a multiplicative QDM approach was employed, applying a standard trace threshold of 0.1 mm/day to stabilize correction factors and define discrete dry-day mass points, a necessary step for accurate soil hydrology modeling in LPJ-GUESS. Other lower-bounded variables, including surface wind speed, relative humidity, and solar radiation, were also corrected globally across the annual distribution.

Temperature variables (T_{min}, T_{mean}, T_{max}) required specialized treatment to preserve the diurnal temperature range (DTR), which heavily dictates fuel moisture evaporation. Additive QDM was applied on a month-by-month basis. This monthly stratification prevented “all-seasons pooled ECDF” artifacts, wherein winter days and summer nights might otherwise be mapped across overlapping historical probability distributions, thereby artificially flattening the DTR. Because QDM corrects variables independently, minor statistical divergences can occasionally cause physical inversions (e.g., $T_{min} > T_{mean}$). To ensure thermodynamic stability within the LPJ-GUESS soil heat flux and snowpack modules, standard physical consistency rules were enforced pixel-by-pixel as a post-processing step, mathematically constraining daily temperatures such that $T_{min} \leq T_{mean} \leq T_{max}$. This comprehensive pipeline yielded physically consistent, CF-compliant forcing datasets that fully preserve the GCM climate change signals at the extreme tails of the distribution.

2.4.2 Soil

LPJ-GUESS requires a soil dataset reflecting soil percolative properties. Using the R programming language and geospatial software, this dataset was constructed at 9 km resolution with data from the

https://doi.org/10.5194/egusphere-2026-1498
Preprint. Discussion started: 8 April 2026

National Soil Dataset for Türkiye and the Harmonized World Soil Database (HWSD v.2.0; FAO & IIASA, 2023) for the neighboring regions.

2.4.3 Drought Analysis

Because LPJ-GUESS–SIMFIRE–BLAZE simulates natural fire potential strictly as a function of biophysical and climatic drivers, an independent assessment of regional hydroclimate was required to contextualize the simulation results. Specifically, to explain the timing of simulated wildfire episodes and to understand the spatial divergences between climate-driven simulations and human-influenced observations, trend analyses of the Standardized Precipitation Evapotranspiration Index (SPEI) at multiple temporal scales were conducted. This allowed for an assessment of how cumulative drying in preceding years influences vegetation conditions and, consequently, wildfire risk.

Unlike simple precipitation metrics, SPEI accounts for the influence of temperature (through potential evapotranspiration), making it a critical tool for identifying climate-change-induced drying. SPEI datasets at 1, 3, 6, 9, 12, 24, and 48-month resolutions were obtained from the ERA5 reanalysis (0.25° spatial resolution). The analysis period was extended to 1991–2025 – predating the burned area record – to capture the cumulative effects of antecedent drying on fuel characteristics and to detect long-term shifts in the regional moisture balance.

Monotonic trends were assessed using the non-parametric Mann–Kendall test, with magnitudes estimated via Sen's slope. To account for serial correlation inherent in hydroclimatic time series, Hamed–Rao modification was applied, and a False Discovery Rate (FDR) correction was enforced to minimize false positives among significant grid cells. The results were visualized through spatial trend maps and Hovmöller diagrams to illustrate the latitudinal evolution of drought for the study area over time. Additionally, drought persistency was evaluated by mapping the frequency of severe (SPEI ≤ -1.5) and extreme drought (SPEI ≤ -2.0), and by calculating inter-index correlations with lags of 0, 6, and 12 months.

2.4.4 Burned Area

Burned area (BA), used for comparative analyses with simulation results, was quantified using the MODIS Collection 6.1 MCD64A1 product (Giglio et al., 2021). This dataset provides pixel-level burn detections at approximately 500 m resolution, identifying burned pixels based on changes in surface reflectance and

https://doi.org/10.5194/egusphere-2026-1498
Preprint. Discussion started: 8 April 2026

thermal anomalies. These detections were aggregated to the study's master grid in the WGS84 spatial reference (EPSG:4326) to align with LPJ-GUESS simulations. Grid cell areas were explicitly calculated using the ellipsoidal area function in the *terra* R package to account for the latitudinal variation in cell size inherent to geographic coordinate systems.

BA was temporally aggregated to monthly intervals by assigning pixels to their detection year and month. These monthly fields were summed annually, and the final outputs were exported in comma-separated values (CSV) format to facilitate spatial analysis in ArcGIS. To ensure consistency with parallel analyses using other datasets (e.g., FireCCI), quality assurance (QA) filtering was evaluated but not enforced beyond the default classification. Sensitivity testing showed that restricting analysis to higher-confidence detections produced negligible differences in regional BA totals, indicating that QA filtering does not materially alter large-scale BA estimates for the study area.

To assess observational uncertainty, MCD64A1 was cross-validated against the gridded FireCCI51 (MODIS-derived for years 2002–2020; Lizundia-Loiola et al., 2020) and FireCCIS311 (Sentinel-derived for years 2019–2024; Chuvieco et al., 2024). While all three products exhibited identical interannual trends, FireCCI algorithms proved significantly more conservative in this region, consistently estimating lower total BA than MCD64A1 (Fig. A3). Given the likelihood of omission errors in conservative algorithms over discontinuous fuel beds, MCD64A1 was selected as the primary benchmark for model evaluation.

For aggregation of burned area by ecoregion, the Terrestrial Ecoregions of the World dataset by Dinerstein et al. (2017; data available from WWF, 2017) was used, cropped to the study domain in geospatial software and imported to RStudio for further analyses.

3. Results

Results are presented in three stages. First, the ability of LPJ-GUESS–SIMFIRE–BLAZE to reproduce historical fire regimes is evaluated against satellite observations (MCD64A1, 2001–2024), with emphasis on interannual variability, biome-specific biases, and fire persistence. This historical benchmarking uses both sets of simulations in its comparisons: those forced by phased historical reanalysis (ERA5-Land), and those forced by the Quantile Delta Mapping (QDM) bias-corrected GCM ensemble median.

https://doi.org/10.5194/egusphere-2026-1498
Preprint. Discussion started: 8 April 2026

Second, observed hydroclimatic trends are examined to establish the regional drought signal that drives fire activity in the northeastern Mediterranean. Finally, building on this evaluation, model projections are used to explore potential changes in burned area (BA), fuel characteristics, and fire return intervals under a high-emissions climate scenario (SSP5-8.5).

3.1 Evaluation of Fire Regimes during the Satellite Era (2001–2025)

3.1.1 Biome-specific magnitude and model performance

LPJ-GUESS simulations, driven by both historical reanalysis and the GCM ensemble median, reveal systematic fire-regime-dependent divergences when compared to MODIS satellite observations. Despite the central tendency of the GCM ensemble results – maintaining an observation/simulation bias ratio close to 1.0 – these divergences point to the difference between simulated natural (climate-driven) fire potential and observed fire activity (including human interference), particularly in arid and semi-arid ecoregions (Fig. 3). Mediterranean ecosystems exhibit the closest agreement between simulated and observed burned area, with median LPJ-GUESS/MODIS ratios near unity. In contrast, steppe and desert ecosystems display a much wider spread in simulated-to-observed ratios, a large interquartile range, and frequent overestimation despite an accurate median agreement. While the model/observation bias ratio for the forest ecoregions lies closer to 1.0 in the GCM ensemble results, both simulations still show moderate overestimation relative to MODIS observations. This pattern is consistent with the absence of explicit fire

https://doi.org/10.5194/egusphere-2026-1498
Preprint. Discussion started: 8 April 2026

291 suppression in the experimental design, allowing simulated fire activity to reflect potential flammability under
292 climatic and vegetation controls alone.

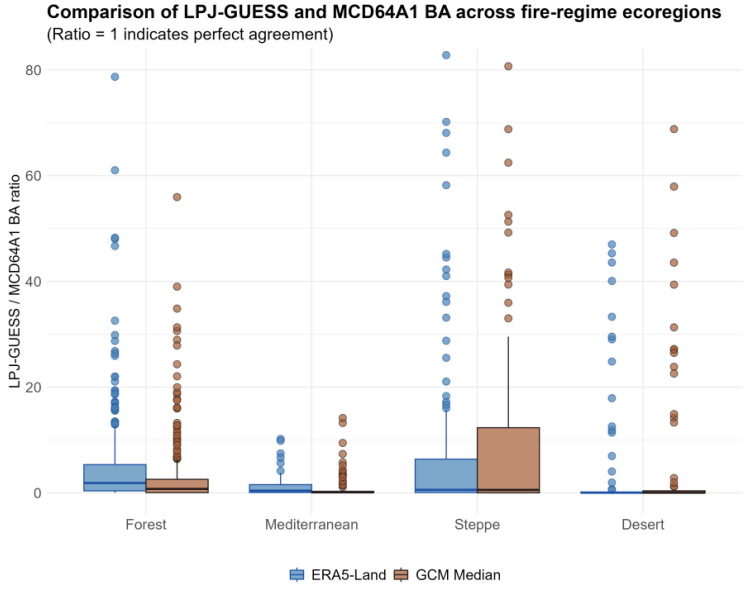

293 **Figure 3.** Distribution of simulated-to-observed burned area ratios grouped by biome. Mediterranean
294 ecoregions show closer agreement with observations, while steppe ecosystems exhibit larger spread and
295 systematic overestimation.

296 For the steppe ecosystems, the overestimations are particularly evident in ecoregions such as the Zagros
297 Mountains forest steppe and the Eastern Anatolian montane steppe, where anthropogenic land use and
298 landscape modification (e.g., agriculture, grazing, and fire management) strongly influence fire activity (Fig.
299 4; for all ecoregions and the reference table: Fig. A1 and Table A1). In these ecoregions, simulated burned
300 area remains consistently higher than MODIS observations, indicating that the model maintains persistent
301 climate-driven fire potential while observed burned area reflects more constrained fire activity. Conversely,
302 during years with strong climatic forcing, ensemble simulations and observations converge, as in 2010, a

https://doi.org/10.5194/egusphere-2026-1498
Preprint. Discussion started: 8 April 2026

pronounced fire year for the Zagros and Eastern Anatolian regions, coinciding with documented regional heatwave conditions and climate anomalies (Heidarlou et al., 2024).

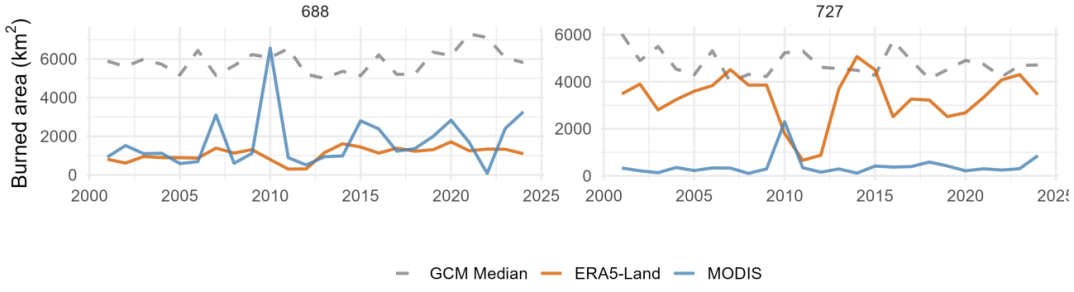

Figure 4. Historical burned area trajectories across semi-arid ecoregions. Comparison of annual BA (km²) simulated by LPJ-GUESS (ERA5-Land orange, GCM ensemble median grey) versus observed by MODIS MCD64A1 (blue) for Zagros Mountains forest steppe [688] and Eastern Anatolian montane steppe [727] ecoregions. Simulation results for the GCM ensemble median show a significant and steady overshoot, except for 2010.

In contrast, several steppe and desert ecoregions display pronounced spikes in observed burned area that are not reproduced by either the reanalysis-driven simulations or the GCM ensemble results. This pattern is evident in Central Anatolian and Pontic steppe landscapes, as well as parts of the Caspian lowland desert ecoregion, where MODIS observations show dynamic fluctuations in burned area while simulated burned area values remain stable and low. The peaks in the satellite record coincide with agricultural regions where post-harvest stubble burning is common, suggesting that these spikes reflect anthropogenic ignitions within cropland mosaics rather than climate-driven wildfire activity.

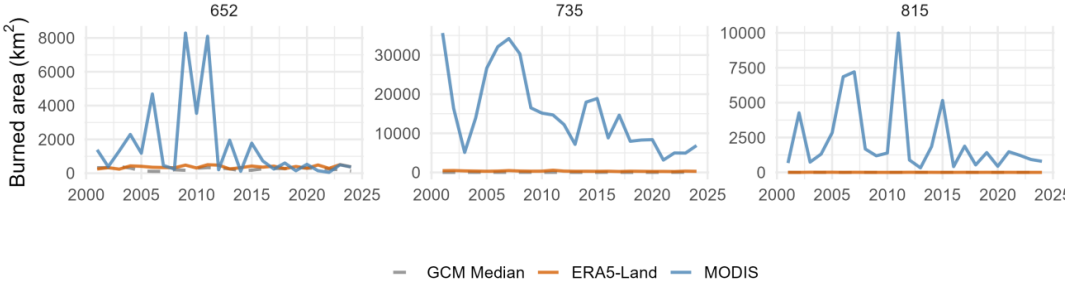

Figure 5. Historical burned area trajectories across arid/semi-arid ecoregions. Comparison of annual BA (km²) simulated by LPJ-GUESS (ERA5-Land orange, GCM ensemble median grey) versus observed by MODIS MCD64A1 (blue) for Central Anatolian steppe and woodlands [652], Pontic steppe [735], and Caspian lowland desert [727] ecoregions. MODIS observations show a continuous overshoot where simulation results record minimal wildfire activity. These ecoregions coincide with cropland mosaics.

https://doi.org/10.5194/egusphere-2026-1498
Preprint. Discussion started: 8 April 2026

A similar divergence appears in the Syrian xeric grasslands and the Mesopotamian shrub desert ecoregions. Here, MODIS observations exhibit an anomalous spike around 2019, while simulations remain comparatively low. This increase coincides with the period of regional instability associated with the Syrian civil war, suggesting that the satellite-detected burned area may result from conflict-related disturbances rather than climate-driven wildfires.

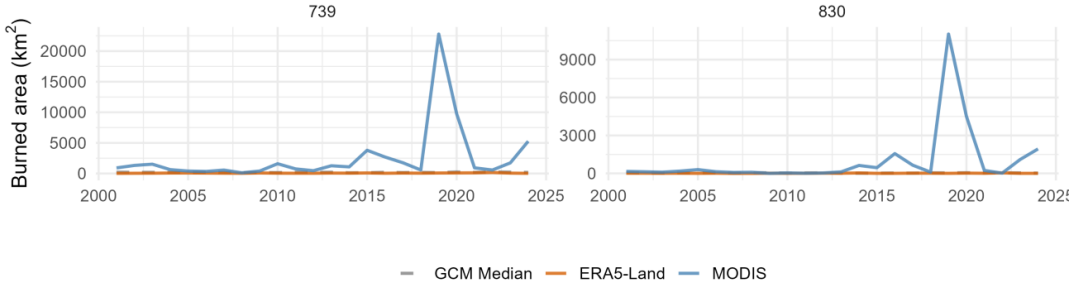

Figure 6. Historical burned area trajectories across arid ecoregions. Comparison of annual BA (km^2) simulated by LPJ-GUESS (ERA5-Land orange, GCM ensemble median grey) versus observed by MODIS MCD64A1 (blue) for Syrian xeric grasslands and shrublands [739] and Mesopotamian shrub desert [830] ecoregions. The spike in 2019 in MODIS observations coincides with the 2019 Syrian civil war.

Consequently, these spatial heterogeneities contribute to weak overall agreement in long-term mean annual burned area across the full domain (Spearman $\rho = 0.17$ for ERA5, $\rho = 0.15$ for the GCM median, Fig. A2). However, comparisons of total annual burned area indicate that simulated magnitudes remain broadly consistent with satellite-based estimates. In particular, the GCM ensemble median closely follows the observed totals and occasionally approaches values derived from Sentinel-based burned area products (Fig. A3). Taken together, these results indicate that while the model reproduces the overall magnitude and biome-scale structure of burned area across the Eastern Mediterranean, local anthropogenic influences strongly shape the spatial distribution of fire activity observed in satellite records.

3.1.2 Interannual variability and validation

Despite the spatial biases described above, the simulations demonstrate measurable skill in reproducing the timing of fire activity. Interannual variability in burned area shows generally positive correlations with satellite observations across ecoregions, indicating that the model captures portions of the year-to-year variability in fire occurrence (Fig. 7). Both the ERA5-driven simulations and the GCM ensemble median exhibit similar distributions of Spearman correlations, with median correlation values modest but positive,

https://doi.org/10.5194/egusphere-2026-1498
Preprint. Discussion started: 8 April 2026

indicating several regions displaying stronger agreement between simulated and observed annual burned area. This pattern suggests that large-scale climatic variability captured in the forcing datasets contributes to the timing of high-fire years in the simulations, even where the spatial magnitude of burned area differs from observations.

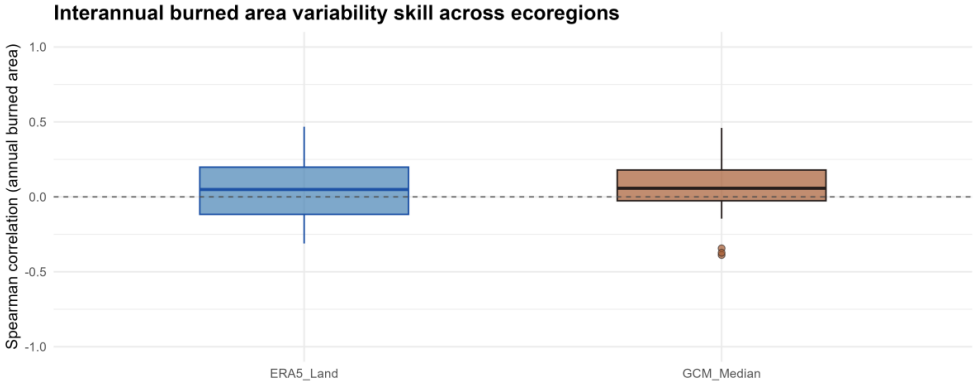

Figure 7. Interannual burned area variability across ecoregions. Spearman correlation coefficients quantifying the agreement between simulated and observed annual burned area time series across ecoregions.

3.1.3 Capture of extreme events and fire persistence

While interannual correlations remain modest across ecoregions, the simulations demonstrate stronger skill in identifying the timing of major fire episodes. Comparison of peak fire years between simulations and observations shows non-random agreement across ecoregions (Fig. A4). The median absolute difference in peak fire year is approximately 7 years, with 25% of ecoregions differing by fewer than 3 years. This temporal alignment is further illustrated in Figure 8, which compares annual burned area trajectories across a set of ecologically diverse forest ecoregions spanning Mediterranean, montane, and transitional systems.

In Mediterranean systems such as the Cyprus Mediterranean forests [790] and the Southern Anatolian montane conifer and deciduous forests [804], the model captures the timing of major fire episodes, including peaks in the late 2000s and around 2020, although simulated burned area generally exceeds observed values. In the Euxine-Colchic broadleaf forests [665], simulations driven by ERA5-Land, and occasionally by the GCM ensemble median, indicate consistently higher fire activity than observed in the satellite record.

https://doi.org/10.5194/egusphere-2026-1498
Preprint. Discussion started: 8 April 2026

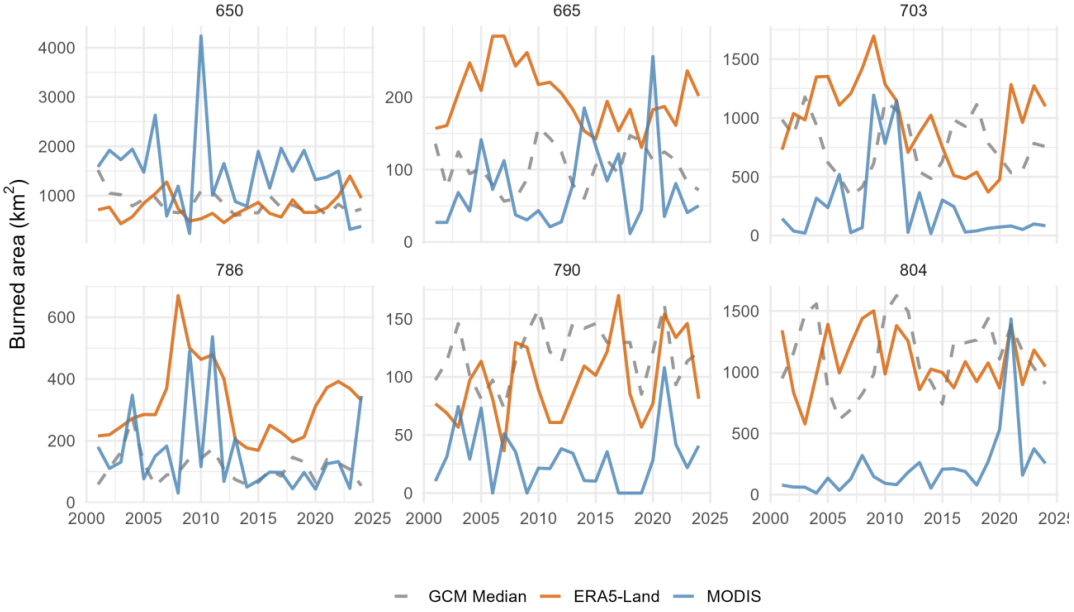

Figure 8. Historical burned area trajectories across forest ecoregions. Comparison of annual BA (km^2) simulated by LPJ-GUESS (ERA5-Land orange, GCM ensemble median grey) versus observed by MODIS MCD64A1 (blue) for six ecologically distinct regions. (Top Row) Caucasus mixed forests [650], Euxine-Colchic broadleaf forests [665], and Northern Anatolian conifer and deciduous forests [703]. (Bottom Row) Anatolian conifer and deciduous mixed forests [786], Cyprus Mediterranean forests [790], and Southern Anatolian montane conifer and deciduous forests [804].

In montane and transitional regions such as the Anatolian conifer and deciduous mixed forests [786], the model reproduces background levels of fire activity as well as periodic increases in burned area. The GCM ensemble median generally follows the timing of observed burned area and, on occasion, the magnitude, while the ERA5-Land simulation tends to produce larger burned areas but captures the overall temporal trend. In the Southern Anatolian montane conifer and deciduous forests [804], the peak fire year of 2021 is reproduced in both simulation datasets. Lower burned area levels observed during much of the remaining period likely reflect the influence of fire suppression. A similar pattern is visible in the Cyprus Mediterranean forests [790].

In addition to reproducing the timing of major fire episodes, the simulations capture the strong spatial concentration of fire activity across the region. Analysis of observed burned area indicates that extreme fire years are disproportionately associated with a limited subset of ecoregions, as illustrated by the Fire Dominance Index (Fig. A5). Several regions exhibit consistently elevated frequencies of high-burned-area

https://doi.org/10.5194/egusphere-2026-1498
Preprint. Discussion started: 8 April 2026

years, effectively functioning as regional “pyro-catchments” where fire activity repeatedly concentrates. This persistence indicates that the model captures the landscape and climatic conditions associated with recurrent fire activity across the Eastern Mediterranean.

Overall, LPJ-GUESS historical simulations reproduce the climatic envelope and domain-scale magnitude of burned area across the Eastern Mediterranean, while spatial discrepancies primarily reflect the influence of anthropogenic land management and fire suppression, which are absent from the experimental design.

3.2 Hydroclimatic Drivers of Fire Activity

3.2.1 Regional drought trends

Trend analysis of the ERA5-Land reanalysis data (1991–2025) revealed a strong and spatially coherent drought signal across the majority of the study region at all temporal scales. Negative SPEI trends emerged around 2008 and persisted through the remainder of the record, becoming stronger from 2015 onwards (Fig. 9b). This intensification was most pronounced at longer accumulation periods (e.g., SPEI-48), indicating a structural shift toward hydrologic deficit rather than merely seasonal variability (Fig. 9a). Parallel drying patterns were observed across all shorter temporal scales (SPEI-1 through SPEI-24; Figs. S9 and S10).

3.2.2 Coupling with fire activity

The spatial distribution of this drying trend aligned closely with the region’s fire regime. Areas exhibiting statistically significant negative SPEI trends (Fig. 9a) generally coincided with zones of elevated burned area (BA) observed in the MCD64A1 record (2001–2024). Furthermore, the spatial persistence of severe drought conditions (SPEI < -2.0) between 1991 and 2025 was particularly evident in parts of the study area characterized by high clustering of BA (Fig. 9c).

Lagged correlation analyses between intermediate (SPEI-06 to SPEI-12) and longer-term drought indices (SPEI-24 to SPEI-48) further revealed similar spatial patterns of drought persistence (Figs. S8–S10). Together, these results indicate a persistent and intensifying drought signal across fire-prone portions of the study domain, providing the hydroclimatic backdrop against historical fire activity and establishing the baseline necessary to interpret the divergences between the simulations and observations.

https://doi.org/10.5194/egusphere-2026-1498
Preprint. Discussion started: 8 April 2026

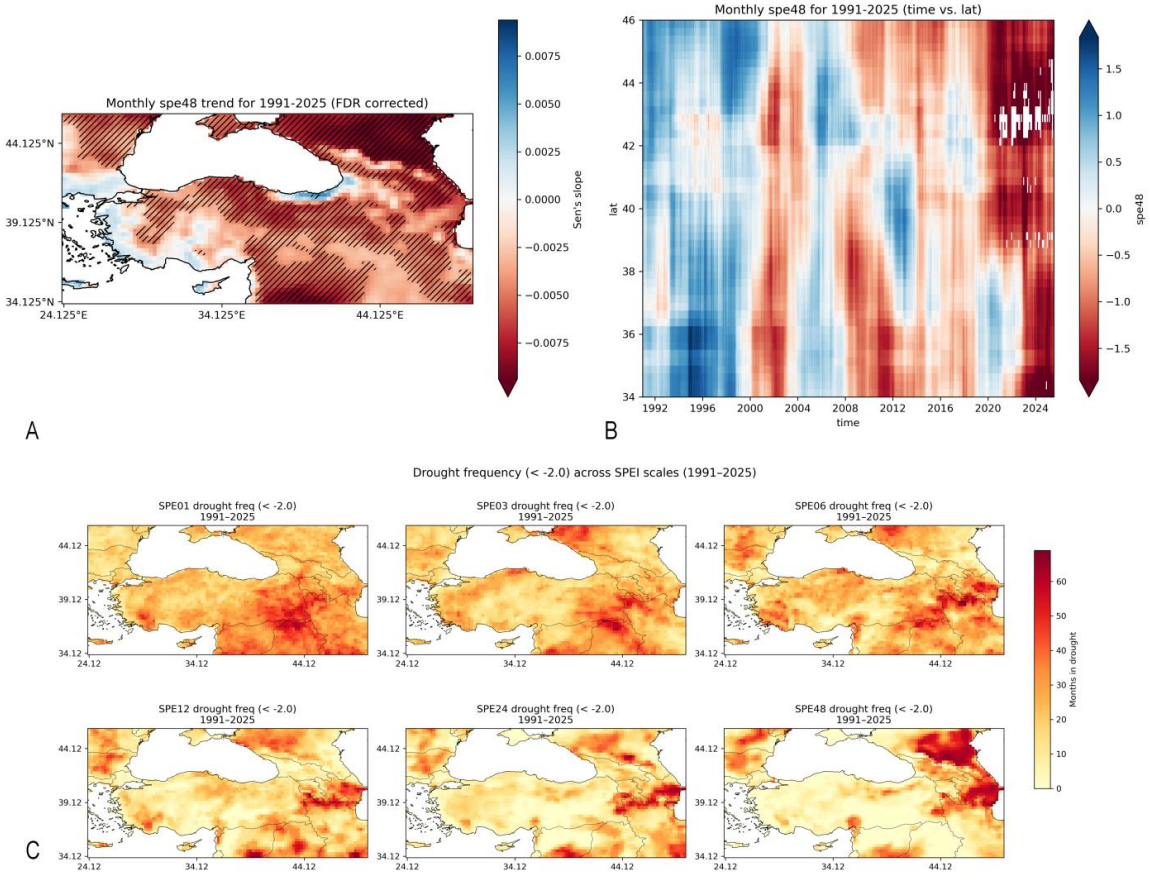

Figure 9. Intensification of regional drought conditions (1991–2025). (a) Spatial distribution of the trend in long-term drought (SPEI-48) using Sen's slope estimator. Hatched areas indicate statistically significant trends ($p < 0.05$), highlighting a broad drying signal across the northeastern Mediterranean. (b) Hovmöller diagram (Time vs. Latitude) of monthly SPEI-48, illustrating the temporal shift from wetter conditions (blue) to persistent, severe drying (red) beginning circa 2008 and intensifying after 2015. (c) Frequency of severe drought months (SPEI ≤ -2.0) across varying accumulation periods (1–48 months). Note the spatial concentration of high drought frequency in the southern and eastern sectors of the domain, coincident with regions of high fire recurrence.

3.3 Long-term fire and vegetation trajectories (1961–2100)

To assess potential future risks relative to the historical trajectory, the simulation period from 1961 to 2100 was analyzed. This timespan encompasses the historical baseline (1961–2014) and the projected response under the high-emissions SSP5-8.5 scenario (2015–2100). Overall, projected changes in vegetation productivity and fire dynamics reveal a heterogeneous reorganization of fire regimes across the Eastern Mediterranean region.

https://doi.org/10.5194/egusphere-2026-1498
Preprint. Discussion started: 8 April 2026

3.3.1 Vegetation productivity and fire probability

Simulated vegetation productivity, represented by the maximum annual fraction of absorbed photosynthetically active radiation (FAPAR), shows a pronounced increase in the highland regions of the study area by the end of the century (Fig. 10a). A strong increase with full vegetation connectivity can be seen in northern Anatolia, along the Black Sea coast. In contrast, the largest increases in maximum fire probability occur primarily in the interior arid and semi-arid regions, including south-central Anatolia and northern Mesopotamia (Fig. 10b). These areas exhibit high projected fire probability maxima despite relatively modest increases in FAPAR, indicating that climatic drivers of fire weather dominate over fuel availability in these landscapes.

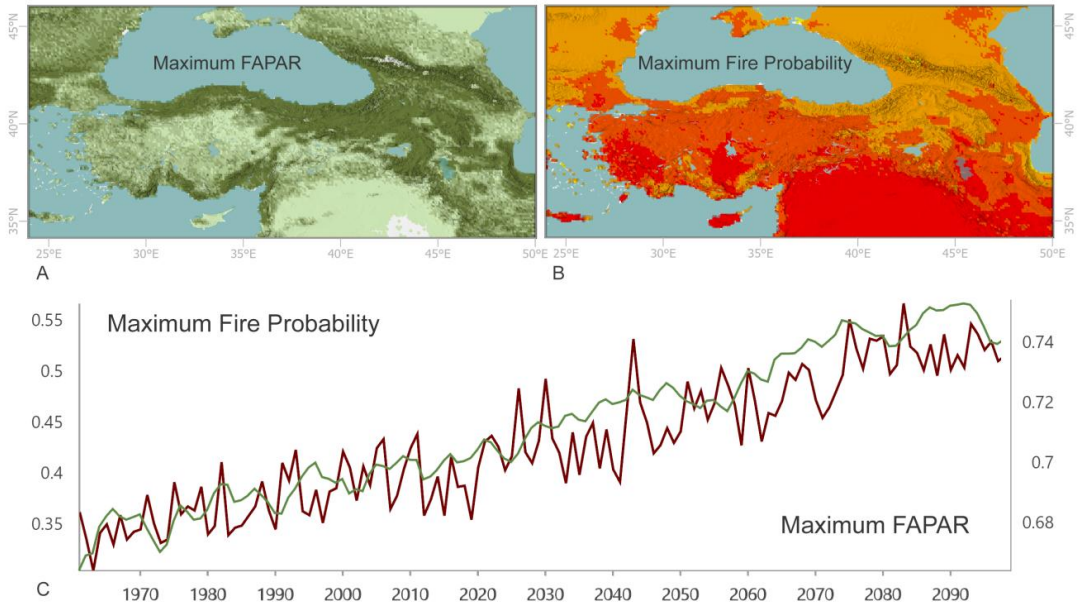

Figure 10. Projected shifts in vegetation and fire probability (1961–2100). (a) Spatial distribution of cumulative maximum FAPAR (Fraction of Absorbed Photosynthetically Active Radiation) simulated under SSP5-8.5, indicating regions of high fuel continuity. (b) Spatial distribution of cumulative maximum fire probability, highlighting the high-risk zones in western and central Anatolia, Cyprus, and the Middle East. (c) Regional time series of maximum FAPAR (green) and maximum fire probability (red). Note the synchronous rise in both metrics towards 2100, suggesting that future fire regimes could be driven by abundant fuel loads interacting with increased ignition probability, potentially leading to significantly shorter fire return intervals.

In the northeastern highlands, where the Northern Anatolian Mountains transition into the Caucasus range, maximum fire probability remains comparatively modest despite high vegetation productivity. A similar

https://doi.org/10.5194/egusphere-2026-1498
Preprint. Discussion started: 8 April 2026

pattern is observed across parts of the Taurus Mountains, where FAPAR increases but fire probability remains spatially heterogeneous. These patterns suggest that topographic and climatic factors continue to limit the conditions necessary for large fire events in these high-elevation systems.

3.3.2 Changes in fire return intervals

Projected fire return intervals (FRI) indicate an overall increase in fire frequency across large parts of the region (Fig. 11). At the beginning of the simulation period, highland systems such as the eastern Anatolian highlands, the Caucasus, the Zagros Mountains, and the Taurus Mountains already exhibit relatively short FRI compared with the surrounding lowlands.

By the end of the century, substantial reductions in FRI emerge across several semi-arid regions. In particular, parts of southern Central Anatolia and the Zagros steppe regions transition from historically long fire return intervals (approximately 30 years) to much more frequent fire regimes, with projected intervals approaching one to two years. In contrast, high-elevation systems such as the Taurus Mountains exhibit comparatively stable FRI over the simulation period. These regions already experience relatively frequent fires in the historical period, and projected changes in fire frequency remain modest relative to those observed in the interior semi-arid zones.

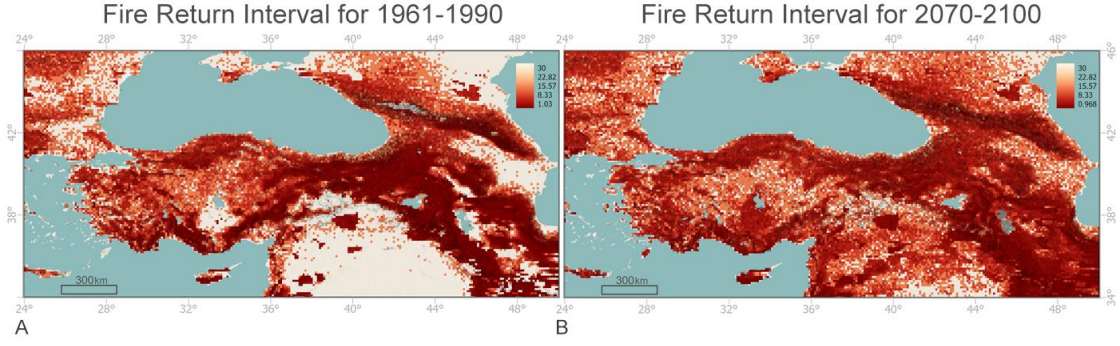

Figure 11. Projected intensification of fire cycles under SSP5-8.5. Comparison of the Fire Return Interval (FRI) in years between the historical baseline (1961–1990, left) and the end-of-century projection (2070–2100, right). Darker red colors indicate shorter return intervals (higher fire frequency). Note the significant shortening of intervals in the historically fuel-limited Central Anatolian and northern Mesopotamian regions, indicating a transition toward more frequent fire activity.

3.3.3 Regional burned area trajectories

https://doi.org/10.5194/egusphere-2026-1498
Preprint. Discussion started: 8 April 2026

Despite the projected increases in fire probability and fire frequency across parts of the region, the simulated median burned area across the Northeast Mediterranean remains relatively stable over the course of the simulation (Fig. 12). After a gradual rise during the late twentieth century, regional burned area exhibits a mild decline toward the end of the twenty-first century.

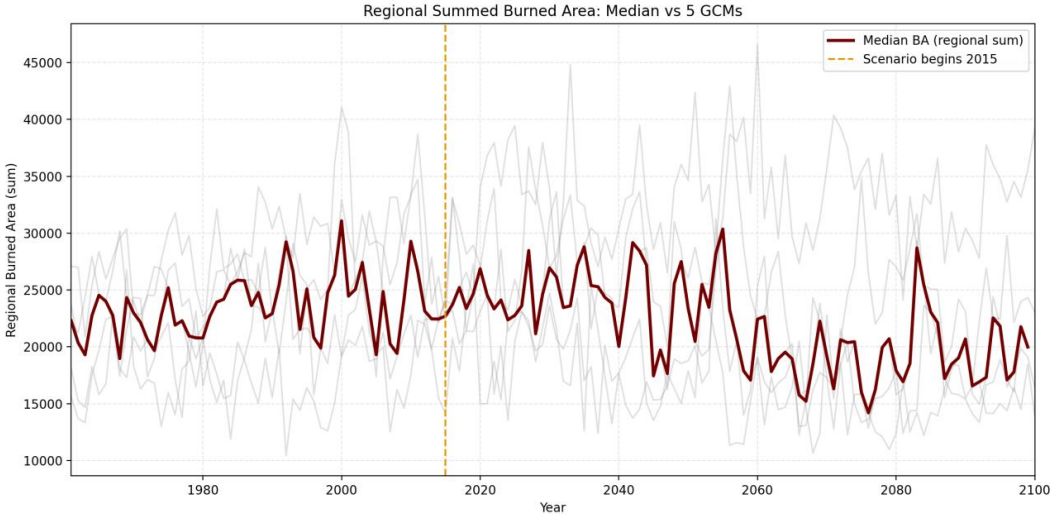

Figure 12. Future burned area trajectories under SSP5-8.5. Time series of regional summed annual BA (km^2) from 1961 to 2100. Grey lines represent individual ensemble members from five bias-corrected GCMs; the dark red line represents the ensemble median. The vertical dashed line marks the start of the future scenario (2015). Despite high interannual variability, the projections indicate a sustained regime of elevated fire activity throughout the century without a monotonic surge in total area burned.

Uncertainty among climate model projections remains substantial, however. While the ensemble median indicates relatively stable burned area, individual GCM members show considerable spread, with some simulations projecting substantially higher burned area toward the end of the century, while others remain closer to the ensemble median. These results indicate that regional burned area trends are strongly influenced by spatial heterogeneity in fire regime responses across the study region.

3.3.4 Spatial redistribution of fire activity

Spatial patterns of projected fire regime change further highlight this regional heterogeneity (Fig. 13). Interior semi-arid regions, particularly Central Anatolia and northern Mesopotamia, exhibit strong increases in fire probability, with some locations showing increases exceeding 25%. However, these areas do not experience comparable increases in burned area, suggesting that more frequent but spatially limited fires

https://doi.org/10.5194/egusphere-2026-1498
Preprint. Discussion started: 8 April 2026

481 dominate these landscapes. In contrast, the Zagros steppe region shows concurrent increases in both fire
482 probability and burned area, indicating an expansion of fire activity in this transitional landscape.

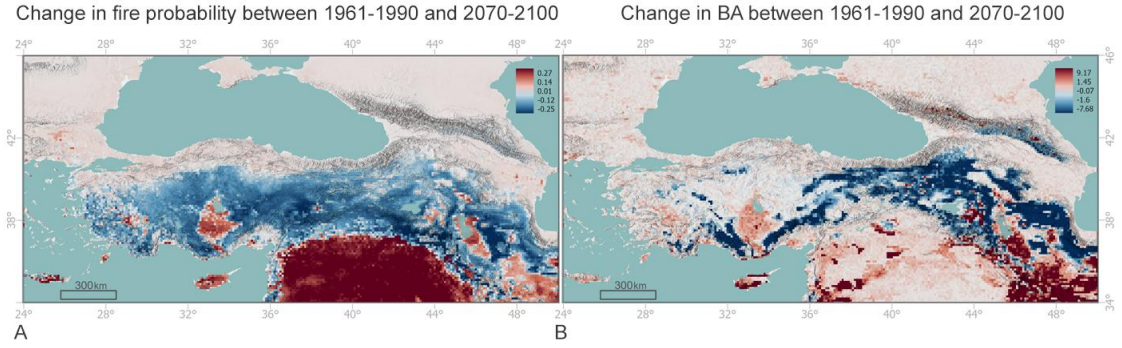

483 **Figure 13.** Projected spatial redistribution of fire activity (2070–2100 vs.1961–1990). (a) Change in mean
484 fire probability. (b) Change in BA (future minus historical) for the GCM ensemble median. Warm colors
485 indicate an increase, highlighting the expansion of risk into southern lowlands.

486 Across parts of the Aegean region, fire probability decreases, whereas some Mediterranean island systems,
487 including Cyprus, show localized increases. In the Taurus Mountains and parts of the eastern Anatolian
488 highlands, simulated burned area declines despite increasing vegetation productivity and relatively stable
489 fire return intervals. These patterns suggest that while fires remain frequent in these mountainous systems,
490 their spatial extent may become more constrained.

491 Together, these simulation results indicate a spatial redistribution of fire regimes across the Eastern
492 Mediterranean, with a potential increase in fire activity concentrated in semi-arid interior regions and parts
493 of the Zagros steppe systems, while several montane forest regions experience more limited fire spread
494 despite increasing vegetation productivity.

495 4. Discussion

496 The simulations presented here suggest that future wildfire dynamics across the Northeast Mediterranean
497 are likely to be shaped less by a uniform intensification of fire activity and more by a spatial redistribution
498 of fire regimes. While rising temperatures and increasing atmospheric dryness elevate fire probability
499 across much of the region, the resulting fire outcomes vary substantially depending on vegetation
500 productivity, topography, and regional hydroclimatic conditions.

https://doi.org/10.5194/egusphere-2026-1498
Preprint. Discussion started: 8 April 2026

One of the most consistent signals emerging from the simulations is the growing importance of semi-arid interior landscapes, particularly Central Anatolia, northern Mesopotamia, and the Zagros steppe regions, as zones of increasing fire potential. In these regions, projected increases in fire probability occur despite relatively modest increases in vegetation productivity. This suggests that future fire regimes in these landscapes may become increasingly governed by climatic fire weather rather than fuel availability alone. The pronounced shortening of fire return intervals in parts of the Central Anatolian and the Zagros steppe ecoregions further indicates that historically infrequent fires may transition toward much more frequent disturbance regimes under continued warming and drying.

In contrast, several montane and northern forested regions exhibit a different trajectory. Along the southern Black Sea coast and across parts of northern Anatolia, simulated vegetation productivity increases substantially, reflecting enhanced growing conditions under warmer climates. However, these increases in fuel availability do not translate into proportional increases in fire probability or burned area. A similar pattern emerges across portions of the Taurus Mountains and the northeastern Anatolian highlands, where fire probability remains spatially heterogeneous despite increasing FAPAR. These results suggest that topographic complexity, cooler microclimates, and moisture availability may continue to constrain the spread of large fires in high-elevation systems, even as vegetation productivity increases.

Taken together, these patterns indicate that future fire regimes in the region may become more heterogeneous, with expanding fire activity in semi-arid transition zones and comparatively stable or spatially constrained fire regimes in several mountainous forest systems. This divergence between fire probability, fire frequency, and burned area highlights the importance of considering multiple fire regime metrics simultaneously when assessing future wildfire risk.

An additional notable feature of the projections is that regional burned area does not increase uniformly despite rising fire probability. The ensemble median suggests relatively stable or slightly declining burned area toward the end of the century, although individual climate model realizations exhibit substantial spread. This outcome likely reflects the spatial redistribution of fire activity across the region, where increases in fire frequency in some semi-arid landscapes are offset by reduced fire spread or more spatially limited fires in several forested mountain regions.

https://doi.org/10.5194/egusphere-2026-1498
Preprint. Discussion started: 8 April 2026

Overall, the simulations point toward a reorganization rather than a simple intensification of fire regimes across the Northeast Mediterranean, with important implications for ecosystem resilience, land management, and future wildfire risk.

4.1 The "Human Gap": Interpreting model–observation divergences in managed landscapes

Comparison between LPJ-GUESS–SIMFIRE–BLAZE simulations and satellite-derived burned area reveals a consistent pattern: the model captures the temporal variability of fire activity with notable skill, while systematic differences in spatial magnitude emerge across heavily managed landscapes. Rather than representing model failure, these divergences reflect the intentional design of the simulation framework. The simulations presented here isolate the biophysical controls on fire regimes by excluding anthropogenic ignition and suppression processes, which are highly complex and difficult to parameterize reliably. Consequently, the model represents a baseline estimate of the potential natural fire regime, whereas the satellite record reflects the contemporary anthropogenic fire regime shaped by land management, suppression infrastructure, and land-use fragmentation. The difference between these two signals therefore provides a useful diagnostic of the human imprint on regional fire dynamics.

This contrast is particularly visible in forested landscapes, where the model consistently produces higher burned area than satellite observations. In ecoregions such as the Northern Anatolian conifer forests and the Balkan mixed forests, the simulated overestimation of burned area likely reflects a suppression deficit, representing the magnitude of fire activity that current climatic conditions could support in the absence of effective fire suppression. In reality, the majority of these landscapes are heavily managed, and fire response systems across Türkiye and southeastern Europe routinely extinguish small ignitions before they can develop into large fires. While this management success masks the true climatic flammability of these ecosystems, the simulations indicate that these forests remain climatically capable of supporting substantially larger burn rates under favorable fire weather conditions (e.g., Caspian Hyrcanian mixed forests [649] and Euxine-Colchic broadleaf forests [665]). In this sense, the divergence between simulated and observed burned area may be interpreted as a latent "fire debt," representing fire activity that is currently suppressed but could emerge if suppression capacity were overwhelmed during extreme fire seasons.

https://doi.org/10.5194/egusphere-2026-1498
Preprint. Discussion started: 8 April 2026

A complementary warning signal appears in steppe and agricultural transition zones such as the Central Anatolian Steppe [725]. In these landscapes, the model tends to underestimate observed burned area in historical simulations, primarily because LPJ-GUESS represents continuous potential vegetation, whereas the real landscape is fragmented by croplands and infrastructure. Human land use therefore dampens the spread of climate-driven fires while simultaneously elevating anthropogenic fire occurrence. However, this relationship shifts in the future simulation results, where LPJ-GUESS projects a transition toward more frequent, climate-driven fire activity in these regions. Given the current agricultural dominance of these landscapes, this projected shift from fragmented, human-modulated fire regimes toward shorter fire return intervals and more continuous burning represents a substantial and potentially disruptive change in system behavior.

Taken together, these contrasting patterns indicate that human land management currently acts as both a suppressor and redistributor of fire activity across the region, but its ability to buffer against climate-driven fire regimes may become increasingly constrained under future hydroclimatic conditions.

4.2 Hydroclimatic forcing and the role of extreme fire weather

Understanding the divergence between historical simulations requires examining the underlying climate forcing datasets. In several forested ecoregions, simulations forced by historical reanalysis (ERA5-Land) produce substantially higher peak fire activity than simulations forced by the bias-corrected GCM ensemble median (e.g., Rhodope montane mixed forests [678], Carpathian montane forests [692], and Anatolian conifer and deciduous mixed forests [786]). This difference illustrates the sensitivity of the model to acute hydroclimatic extremes.

GCM simulations are designed primarily to capture long-term climate trajectories and large-scale circulation patterns. When multiple GCM outputs are combined into an ensemble median, the resulting signal inherently smooths interannual variability and suppresses extreme anomalies. While this approach provides a robust estimate of long-term climatic trends, it cannot reproduce the exact chronological sequence of weather events experienced by the landscape.

Historical reanalysis, by contrast, represents the chronological climate record that actually occurred during the satellite observation era. In addition to capturing drought severity, it preserves the temporal persistence

https://doi.org/10.5194/egusphere-2026-1498
Preprint. Discussion started: 8 April 2026

and sequencing of hydroclimatic conditions, including multi-year drought development and recovery phases. These dynamics introduce drought legacy effects, whereby antecedent moisture deficits influence vegetation productivity, fuel accumulation, and fuel dryness over timescales longer than a single season.

The strong response of LPJ-GUESS to ERA5-Land forcing therefore demonstrates the internal biophysical consistency of the model. When presented with verified hydroclimatic extremes, the model simulates correspondingly large natural fire potential. The fact that satellite observations often show comparatively low burned area during these same climatic peaks further reinforces the existence of a suppression-mediated fire regime, in which effective fire management prevents many fires from reaching their climatic potential.

4.3 Biophysical mechanisms governing natural fire regimes

Removing anthropogenic influences from the simulations reveals the fundamental biophysical constraints that structure fire regimes across the region. Two contrasting mechanisms emerge: fuel-limited systems, where biomass availability controls fire activity, and climate-limited systems, where fuel is abundant but ignition and spread depend on climatic thresholds.

4.3.1 Fuel-limited hysteresis in closed forest systems

One striking feature of the historical simulations is the behavior of the Caspian Hyrcanian mixed forests [649]. Following simulated peak fire years, the system exhibits a refractory period of several years under ERA5-Land forcing, during which fire activity drops to near zero. This lag is consistent with the time required for understory biomass and fuel continuity to recover after a disturbance event. In this closed-canopy deciduous system, fire activity is therefore not strictly climate-driven; instead, it is strongly fuel-limited. Once available biomass is consumed, the system temporarily loses the capacity to sustain fire spread until vegetation regrowth restores sufficient fuel connectivity. This dynamic contrasts with nearby pine-dominated systems, where rapidly accumulating needle litter maintains a continuously flammable fuel bed capable of responding quickly to drought events.

4.3.2 The “hotter and greener” paradox

https://doi.org/10.5194/egusphere-2026-1498
Preprint. Discussion started: 8 April 2026

A second mechanism emerging from the simulations is the apparent paradox of increasing vegetation productivity under a warming climate. Classical drought theory often predicts that increasing aridity will reduce fuel availability and therefore suppress fire activity. However, the simulations show simultaneous increases in maximum FAPAR and fire probability across several northern and montane regions. This pattern likely reflects the combined influence of CO_2 fertilization and shifts in vegetation composition. Elevated atmospheric CO_2 improves plant water-use efficiency, allowing vegetation productivity to remain stable or even increase despite declining moisture availability. At the same time, warming temperatures may facilitate the expansion of drought-adapted species into previously cooler environments, maintaining canopy density and fuel continuity even under drying conditions. The result is a “hotter and greener” landscape in which the structural prerequisites for fire (fuel abundance) are maintained, while climatic constraints on ignition and spread weaken. This mechanism may be particularly important along the transitional zones of northern Anatolia, where rising productivity coincides with increasing fire probability.

4.4 Spatial redistribution of future fire regimes and implications for fire management

Although the regional burned area signal remains relatively stable, the projected redistribution of fire activity has important implications for fire management. Current fire management strategies in the Northeast Mediterranean prioritize the wildland–urban interface and coastal landscapes where human ignitions dominate. However, the simulations indicate that future fire risk may increasingly emerge from semi-arid interior regions and transitional landscapes, particularly Central Anatolia and northern Mesopotamia. These regions, historically dominated by anthropogenic ignitions and fragmented landscapes, exhibit the strongest projected increases in fire probability and the most pronounced shortening of fire return intervals towards the end of the century.

Another emerging concern is the potential for simultaneous fire activity across large, topographically heterogeneous mountain belts. Currently, the majority of the highland regions in the study area show low fire probability – a contrast that helps explain why the regional median burned area remains relatively stable despite sharp increases in fire probability across semi-arid ecoregions in the south. However, if intensifying and prolonged warming and drying remove these climatic limitations on ignition across wide areas, multiple fires could occur concurrently across diverse ecoregions. Such scenarios could severely challenge existing

https://doi.org/10.5194/egusphere-2026-1498
Preprint. Discussion started: 8 April 2026

suppression systems by exceeding the logistical capacity of firefighting infrastructure, particularly during extreme, prolonged heatwave events.

Changes in fire frequency may also influence long-term vegetation dynamics. A potential increase in the frequency of wildfires in the lowlands may favor the expansion of fire-adapted shrublands and conifer species, potentially creating “fire ladders” that facilitate the upslope spread of high-intensity fires into ecosystems historically less adapted to frequent disturbance. Over longer timescales, such feedbacks could alter the composition and resilience of several Mediterranean and Anatolian forest systems.

5. Conclusion

This study demonstrates that future wildfire dynamics across the Northeast Mediterranean are unlikely to be characterized by a uniform increase in burned area. Instead, the simulations indicate a spatial redistribution of fire regimes, driven by the interaction between hydroclimatic change, vegetation productivity, and landscape structure. While fire probability increases across large parts of the region, particularly in semi-arid interior zones, this does not consistently translate into greater burned area. Rather, shifts in fire frequency, fuel continuity, and topographic constraints lead to divergent regional responses.

By isolating the natural fire potential using LPJ-GUESS–SIMFIRE–BLAZE, this study also highlights the extent to which contemporary fire regimes are shaped by human land management. The contrast between simulated and observed burned area reveals a dual role of human influence: effective fire suppression masks latent climatic flammability in forested systems, while land-use fragmentation constrains fire spread in agricultural landscapes. However, future projections suggest that these buffering effects may become increasingly limited under intensifying hydroclimatic stress and more frequent drought conditions.

Furthermore, the dual forcing approach in this study helps clarify the distinct roles of historical reanalysis versus bias-corrected climate model ensembles in anticipating fire regimes. Temporally explicit historical baselines reveal the critical role of observed drought sequences and legacy effects in priming ecosystems for elevated fire potential. Conversely, while the GCM ensemble median inherently smooths these acute historical extremes, it remains an indispensable tool for projecting centennial trajectories and forewarning of potential systemic, long-term shifts in future risk. Together, these complementary approaches enable a more robust interpretation of both existing mechanisms and future fire dynamics.

https://doi.org/10.5194/egusphere-2026-1498
Preprint. Discussion started: 8 April 2026

Ultimately, these findings suggest that the primary impact of climate change on wildfire in Northeast Mediterranean may not be a simple increase in fire activity, but a fundamental reorganization of where and how fires occur. This has urgent implications for fire management, as emerging risk zones and the increasing simultaneity of fire-conducive conditions across broad geographies threaten to challenge existing suppression strategies. Anticipating future wildfire risk therefore requires moving beyond expectations of uniform intensification and toward a mechanistic understanding of how climate, vegetation, and human land use jointly redistribute fire regimes across space.

https://doi.org/10.5194/egusphere-2026-1498
Preprint. Discussion started: 8 April 2026

APPENDIX

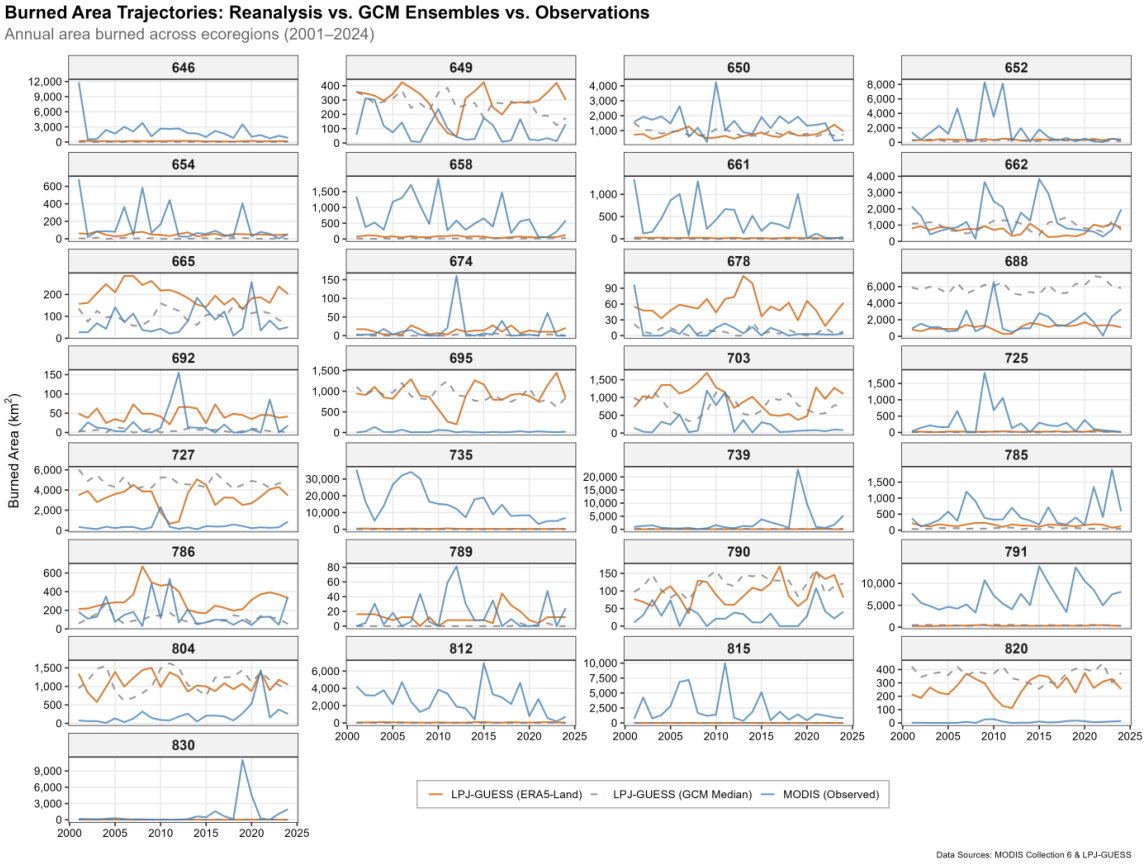

Figure A1. Interannual burned area trajectories across all study ecoregions (2001–2024). Annual burned area (km²) simulated by LPJ-GUESS driven by ERA5-Land (orange) and the GCM ensemble median (grey), compared against MODIS MCD64A1 satellite observations (blue). The plots illustrate the model's heterogenous performance across biomes. While Mediterranean ecoregions demonstrate strong temporal alignment with observations, forested and steppe ecoregions exhibit systematic magnitude offsets. These offsets are consistent with the complex bidirectional influence of anthropogenic fire suppression, agricultural ignitions, and land-use fragmentation, which are intentionally excluded from the natural-potential simulations.

https://doi.org/10.5194/egusphere-2026-1498
Preprint. Discussion started: 8 April 2026

680 **Table A1:** Ecoregion classification. List of WWF terrestrial ecoregions within the study domain, their corresponding
681 numeric ID used in analysis, and their broad biome classification (Forest, Mediterranean, Steppe, or Desert).

ID	Ecoregion Name	Vegetation Type
786	Anatolian conifer and deciduous mixed forests	*Forest*
678	Rodope montane mixed forests	*Forest*
703	Northern Anatolian conifer and deciduous forests	*Forest*
650	Caucasus mixed forests	*Forest*
662	Eastern Anatolian deciduous forests	*Forest*
665	Euxine-Colchic broadleaf forests	*Forest*
649	Caspian Hyrcanian mixed forests	*Forest*
646	Balkan mixed forests	*Forest*
674	Pannonian mixed forests	*Forest*
658	Crimean Submediterranean forest complex	*Forest*
692	Carpathian montane forests	*Forest*
654	Central European mixed forests	*Forest*
804	Southern Anatolian montane conifer and deciduous forests	*Forest*
785	Aegean and Western Turkey sclerophyllous/mixed forests	*Mediterranean*
790	Cyprus Mediterranean forests	*Mediterranean*
791	Eastern Mediterranean conifer-broadleaf forests	*Mediterranean*
789	Crete Mediterranean forests	*Mediterranean*
661	East European forest steppe	*Steppe*
725	Central Anatolian steppe	*Steppe*
688	Zagros Mountains forest steppe	*Steppe*
727	Eastern Anatolian montane steppe	*Steppe*
652	Central Anatolian steppe and woodlands	*Steppe*
735	Pontic steppe	*Steppe*
695	Elburz Range forest steppe	*Steppe*
820	Central Persian desert basins	*Desert*
815	Caspian lowland desert	*Desert*
830	Mesopotamian shrub desert	*Desert*
739	Syrian xeric grasslands and shrublands	*Desert*
812	Azerbaijan shrub desert and steppe	*Desert*

https://doi.org/10.5194/egusphere-2026-1498
Preprint. Discussion started: 8 April 2026

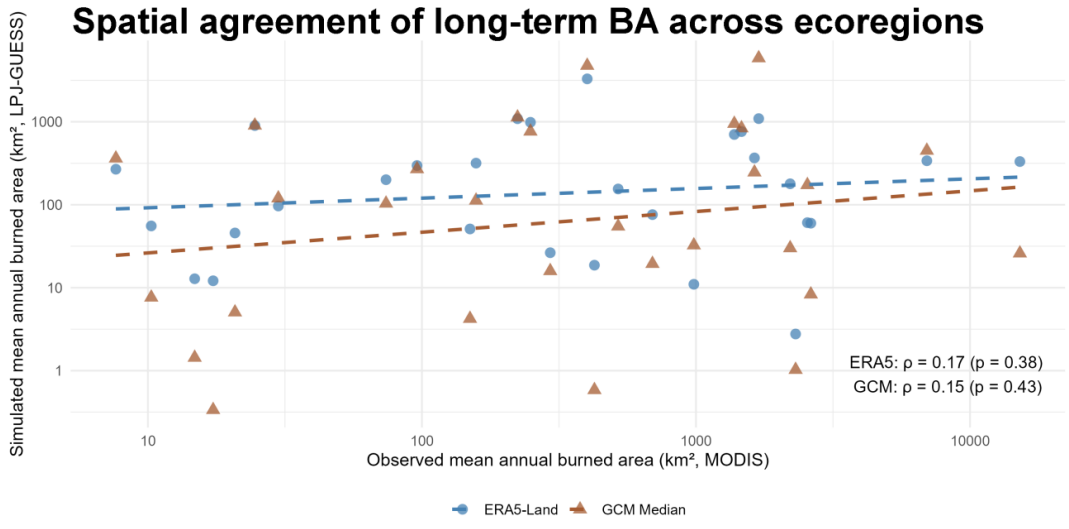

Figure A2. Spatial agreement of long-term burned area. Comparison of mean annual burned area (km2) simulated by LPJ-GUESS–SIMFIRE–BLAZE versus observed by MODIS MCD64A1 across all ecoregions within the study area. The blue dashed line represents linear trend for ERA5-Land simulations and the orange dashed line represents linear trend for the GCM ensemble median. Weak spatial correlations (Spearman rho = 0.17 for ERA5-Land simulation and rho = 0.15 for the GCM ensemble median) highlight the model's limitation in reproducing spatial magnitude heterogeneity driven by local anthropogenic factors, despite capturing temporal variability.

https://doi.org/10.5194/egusphere-2026-1498
Preprint. Discussion started: 8 April 2026

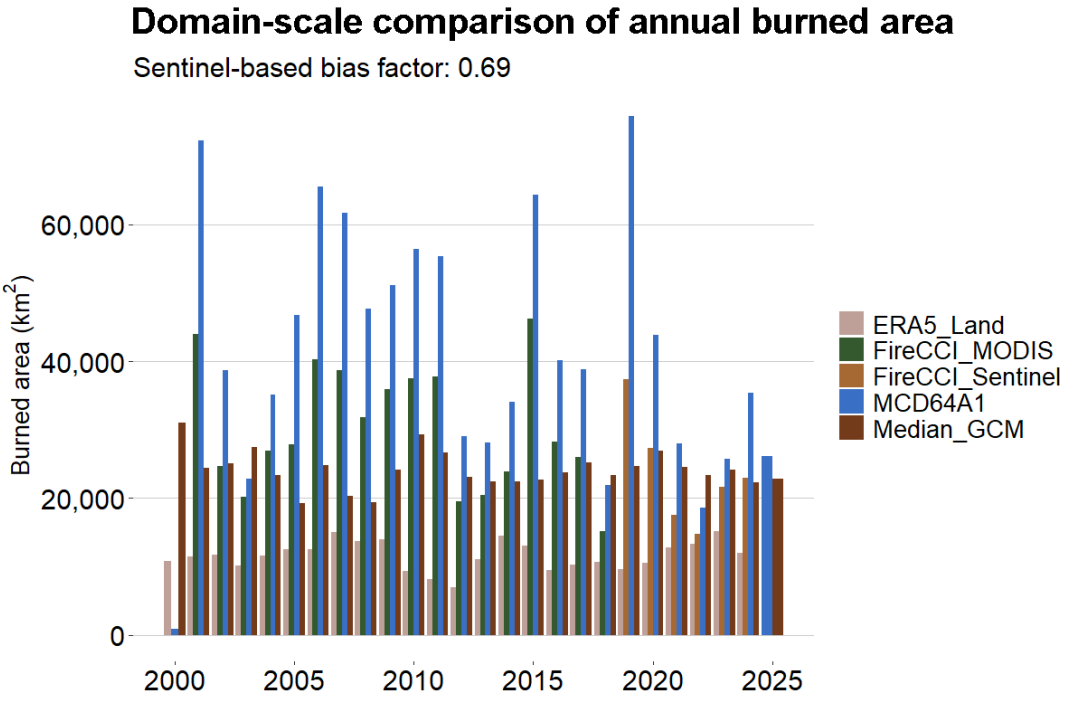

Figure A3. Intercomparison of observational burned area products and simulation results. Annual burned area (BA) totals for the study domain derived from MCD64A1 (blue), FireCCI (orange/green) products, and ERA5-Land (beige) and GCM ensemble median simulation results (dark red). While absolute magnitudes differ – with MCD64A1 consistently detecting more BA than the more conservative FireCCI algorithms – the interannual variability remains highly consistent across all sensor platforms, confirming the robustness of the high-fire years identified in this study.

https://doi.org/10.5194/egusphere-2026-1498
Preprint. Discussion started: 8 April 2026

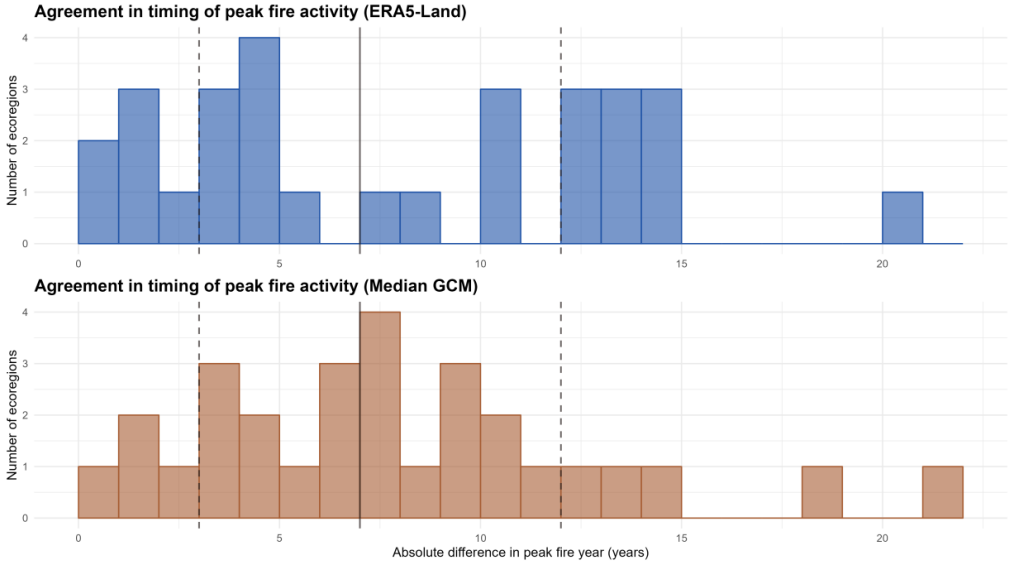

Figure A4. Agreement in timing of peak fire activity. Histogram of the absolute difference (in years) between the observed and simulated peak fire year across all ecoregions from the simulation results of ERA5-Land and the GCM ensemble median. The solid vertical line represents the median difference (7 years). Dashed lines indicate the 25th percentile (difference ≤ 3 years) and 75th percentile, illustrating that for a significant subset of ecoregions, the model successfully captures the broad temporal placement of major fire episodes.

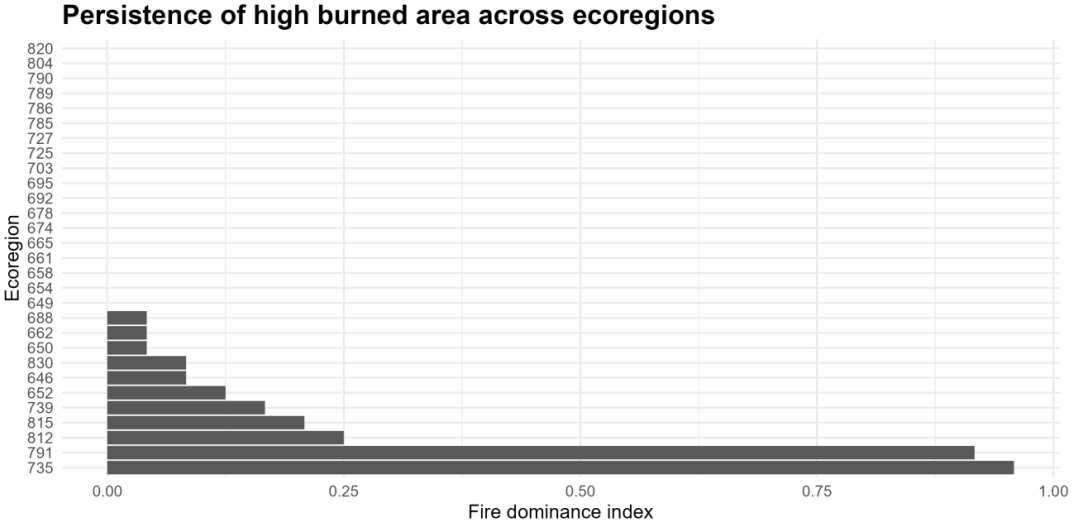

Figure A5. Persistence of high burned-area years across ecoregions. Ecoregions ranked by the Fire Dominance Index, defined as the fraction of years in which annual burned area exceeds the global 90th percentile of the regional burned-area distribution. The results show that extreme fire activity is concentrated in a limited subset of ecoregions, indicating persistent “pyro-catchments” that account for a disproportionate share of regional burned area.

https://doi.org/10.5194/egusphere-2026-1498
Preprint. Discussion started: 8 April 2026

Data Availability

All datasets used in this manuscript for drought, ecoregions, and burned area analyses can be downloaded from their original sources. LPJ-GUESS simulation results are available in Zenodo (embargoed until publication, but available during peer review at: https://tinyurl.com/ForecastingTheFlame) at https://doi.org/10.5281/zenodo.18200254).

Code Availability

The R and Python codes generated and used during the study are part of an ongoing study, but are readily available from the corresponding author by request. LPJ-GUESS dynamic vegetation model's home page is: https://web.nateko.lu.se/lpj-guess/

Acknowledgements

The author wishes to thank the LPJ-GUESS community, the Fire Modelling group, and the developers of the model from the zero hour to the present, for their continuous support and feedback.

Author Contributions

B.E. designed the study and its methodology, curated the data, conceptualized the experimental design, conducted the formal analysis, validated the results, wrote the manuscript and visualized the data.

Competing Interests

The author declares no conflict of interest.

Funding Declaration

Research conducted for this study has been made possible by grant number MGA-2026-47431. Computing resources used in this work were provided by the National Center for High Performance Computing (UHeM) in Turkey, under Grant Number 1007482020.

https://doi.org/10.5194/egusphere-2026-1498
Preprint. Discussion started: 8 April 2026

References

CAL FIRE: 2025 incident archive, California Department of Forestry and Fire Protection, https://www.fire.ca.gov/incidents/2025, 2025.

Chuvieco, E., Pettinari, M. L., Lizundia-Loiola, J., Khairoun, A., Danne, O., Boettcher, M., and Storm, T.: ESA Fire Climate Change Initiative (Fire_cci): Sentinel-3 SYN Burned Area Grid product, version 1.1, NERC EDS Centre for Environmental Data Analysis, https://catalogue.ceda.ac.uk/uuid/da8e669a74334c82a56e0b470bc4ef04, 2024.

Dinerstein, E., Olson, D., Joshi, A., Vynne, C., Burgess, N. D., Wikramanayake, E., Hahn, N., Palminteri, S., Hedao, P., Noss, R., Hansen, M., et al.: An ecoregion-based approach to protecting half the terrestrial realm, BioScience, 67, 534–545, https://doi.org/10.1093/biosci/bix014, 2017.

Duane, A., Castellnou, M., and Brotons, L.: Towards a comprehensive look at global drivers of novel extreme wildfire events, Climatic Change, 165, 43, https://doi.org/10.1007/s10584-021-03066-4, 2021.

Ekberzade, B., Görüm, T., Karabacak, F., et al.: Up in flames: the human factor behind a megafire in Mediterranean Türkiye, npj Natural Hazards, 2, 65, https://doi.org/10.1038/s44304-025-00120-4, 2025.

Ekberzade, B., Yetemen, O., Ezber, Y., Sen, O. L., and Dalfes, H. N.: Latitude or altitude as the future refugium? A case for the future of forests in Asia Minor and its surroundings, Ecology and Evolution, 14, e11131, https://doi.org/10.1002/ece3.11131, 2024.

Ekberzade, B., Yetemen, O., and Sen, O. L.: Looking into a fuzzy future: coupled effect of pyrogeography and a changing climate on an already fragile terrestrial ecosystem, EGU General Assembly 2022, Vienna, Austria, EGU22-239, https://doi.org/10.5194/egusphere-egu22-239, 2022.

Ellis, T. M., Bowman, D. M. J. S., and Williamson, G. J.: Human activity augments lightning ignitions to reshape fire seasonality across all biomes on Earth, Nature Ecology & Evolution, 9, 2069–2079, https://doi.org/10.1038/s41559-025-02862-w, 2025.

FAO and IIASA: Harmonized World Soil Database version 2.0, FAO and IIASA, https://doi.org/10.4060/cc3823en, 2023.

https://doi.org/10.5194/egusphere-2026-1498
Preprint. Discussion started: 8 April 2026

François, B., Teber, K., Brett, L., Leeding, R., Gimeno-Sotelo, L., Domeisen, D. I. V., Suarez-Gutierrez, L., and Bevacqua, E.: Concurrent modes of climate variability linked to spatially compounding wind and precipitation extremes in the Northern Hemisphere, Earth System Dynamics, 16, 1029–1051, https://doi.org/10.5194/esd-16-1029-2025, 2025.

Gelabert, P. J., Jiménez-Ruano, A., Ochoa, C., Alcasena, F., Sjöström, J., Marrs, C., Ribeiro, L. M., Palaiologou, P., Bentué Martínez, C., Chuvieco, E., Vega-Garcia, C., and Rodrigues, M.: Assessing human-caused wildfire ignition likelihood across Europe, EGUsphere [preprint], https://doi.org/10.5194/egusphere-2025-143, 2025.

Giglio, L., Justice, C., Boschetti, L., and Roy, D.: MODIS/Terra+Aqua Burned Area Monthly L3 Global 500m SIN Grid V061 [Data set], NASA Land Processes Distributed Active Archive Center, https://doi.org/10.5067/MODIS/MCD64A1.061, 2021.

Gonzalez, S., and Ghermandi, L.: How to define the wildland-urban interface? Methods and limitations: towards a unified protocol, Frontiers in Environmental Science, 11, 1284631, https://doi.org/10.3389/fenvs.2023.1284631, 2024.

Hantson, S., Arneth, A., Harrison, S. P., Kelley, D. I., Prentice, I. C., et al.: The status and challenge of global fire modelling, Biogeosciences, 13, 3359–3375, https://doi.org/10.5194/bg-13-3359-2016, 2016.

Heidarlou, B. H., Gholamzadeh, B. M., and Borz, S. A.: Unveiling the Role of Climate and Environmental Dynamics in Shaping Forest Fire Patterns in Northern Zagros, Iran, Land, 13, 1453, https://doi.org/10.3390/land13091453, 2024.

Keeping, T., Bergin, C., Pinto, I., Ekberzade, B., and Voulgarakis, A.: Weather conditions leading to deadly wildfires in Türkiye, Cyprus and Greece made 10 times more likely due to climate change [Technical Report], Centre for Environmental Policy, Imperial College London, https://doi.org/10.25560/123302, 2025.

Knorr, W., Kaminski, T., Arneth, A., and Weber, U.: Impact of human population density on fire frequency at the global scale, Biogeosciences, 11, 1085–1102, https://doi.org/10.5194/bg-11-1085-2014, 2014.

https://doi.org/10.5194/egusphere-2026-1498
Preprint. Discussion started: 8 April 2026

Li, F., Val Martin, M., Hantson, S., Andreae, M. O., Arneth, A., et al.: Evaluation of global fire simulations in CMIP6 Earth system models, Geoscientific Model Development, 17, 8751–8773, https://doi.org/10.5194/gmd-17-8751-2024, 2024.

Lizundia-Loiola, J., Otón, G., Ramo, R., and Chuvieco, E.: A spatio-temporal active-fire clustering approach for global burned area mapping at 250 m from MODIS data, Remote Sensing of Environment, 236, 111493, https://doi.org/10.1016/j.rse.2019.111493, 2020.

Newman Thacker, F. E., Bartholomeus, H., Rosell Ibarz, M., and Teuling, A. J.: Characterising land cover—wildfire interactions in Catalonia and their implications for resilience, Fire Ecology, 21, 31, https://doi.org/10.1186/s42408-025-00372-5, 2025.

Nurrohman, R. K., Kato, T., Ninomiya, H., Végh, L., Delbart, N., Miyauchi, T., Sato, H., Shiraishi, T., and Hirata, R.: Future projections of Siberian wildfire and aerosol emissions, Biogeosciences, 21, 4195–4227, https://doi.org/10.5194/bg-21-4195-2024, 2024.

Olson, D. M., Dinerstein, E., Wikramanayake, E. D., Burgess, N. D., Powell, G. V. N., et al.: Terrestrial ecoregions of the world: A new map of life on earth, Bioscience, 51, 933–938, https://10.1641/0006-3568(2001)051[0933:TEOTWA]2.0.CO;2, 2001.

Pellegrini, A. F. A., Reich, P. B., Hobbie, S. E., et al.: Soil carbon storage capacity of drylands under altered fire regimes, Nature Climate Change, 13, 1089–1094, https://doi.org/10.1038/s41558-023-01800-7, 2023.

Rabin, S. S., Melton, J. R., Lasslop, G., Bachelet, D., Forrest, M., Hantson, S., Kaplan, J. O., Li, F., et al.: The Fire Modeling Intercomparison Project (FireMIP), phase 1: experimental and analytical protocols with detailed model descriptions, Geosci. Model Dev., 10, 1175–1197, https://doi.org/10.5194/gmd-10-1175-2017, 2017.

Richardson, D., Black, A. S., Irving, D., et al.: Global increase in wildfire potential from compound fire weather and drought, npj Climate and Atmospheric Science, 5, 23, https://doi.org/10.1038/s41612-022-00248-4, 2022.

San-Miguel-Ayanz, J., Durrant, T., Boca, R., Maianti, P., Libertá, G., Artés-Vivancos, T., Oom, D., Branco, A., de Rigo, D., Ferrari, D., Pfeiffer, H., Grecchi, R., and Nuijten, D.: Advance Report on Forest Fires in

https://doi.org/10.5194/egusphere-2026-1498
Preprint. Discussion started: 8 April 2026

Europe, Middle East and North Africa 2021, Publications Office of the European Union, https://doi.org/10.2760/039729, 2022.

Smith, B., Prentice, I. C., and Sykes, M. T.: Representation of vegetation dynamics in the modelling of terrestrial ecosystems: comparing two contrasting approaches within European climate space, Global Ecology and Biogeography, 10, 621–637, 2001.

Sutanto, S. J., Duku, C., Gülveren, M., Dankers, R., and Paparrizos, S.: Future intensification of compound and consecutive drought and heatwave risks in Europe, Natural Hazards and Earth System Sciences, 25, 3879–3895, https://doi.org/10.5194/nhess-25-3879-2025, 2025.

Wasserman, T. N., and Mueller, S. E.: Climate influences on future fire severity: a synthesis of climate-fire interactions and impacts on fire regimes, high-severity fire, and forests in the western United States, Fire Ecology, 19, 43, https://doi.org/10.1186/s42408-023-00200-8, 2023.

Wood, R. R.: Role of mean and variability change in changes in European annual and seasonal extreme precipitation events, Earth System Dynamics, 14, 797–816, https://doi.org/10.5194/esd-14-797-2023, 2023.

World Weather Attribution: Climate change increased the likelihood of wildfire disaster in highly exposed Los Angeles area, https://www.worldweatherattribution.org/climate-change-increased-the-likelihood-of-wildfire-disaster-in-highly-exposed-los-angeles-area/, 2025a.

World Weather Attribution: Weather conditions leading to deadly wildfires in Türkiye, Cyprus and Greece made 10 times more likely due to climate change, https://www.worldweatherattribution.org/weather-conditions-leading-to-deadly-wildfires-in-turkiye-cyprus-and-greece-made-10-times-more-likely-due-to-climate-change/, 2025b.

World Wildlife Fund (WWF): Terrestrial Ecoregions of the World [Dataset], Data Basin, https://databasin.org/datasets/68635d7c77f1475f9b6c1d1dbe0a4c4c/, 2017.